[Reprinted from BULLETIN OF THE AMERICAN METEOROLOGICAL SOCIETY, Vol. 75, No. 3, March 1994]
Printed in U. S. A.

REBAL '92—A Cooperative Radiation and Energy Balance Field Study for Imagery and Electromagnetic Propagation

Arnold Tunick,*
Henry Rachele,*
Frank V. Hansen,*
Terry A. Howell,+
Jean L. Steiner,+
Arland D. Schneider,+
and Steve R. Evett+

Abstract

The surface energy balance directly affects vertical gradients in temperature and specific humidity within the atmospheric surface layer, and these gradients influence optical turbulence. This study was conducted to improve current understanding of the partitioning of energy at the ground surface of a bare soil field and its influence on the character and intensity of optical turbulence as represented by the refractive index structure parameter, C_n^2, and to improve micrometeorological models of the surface energy balance. The field study entitled "Radiation Energy Balance Experiment for Imagery and Electromagnetic Propagation" was conducted by the United States Army Atmospheric Sciences Laboratory and the United States Department of Agriculture Agricultural Research Service, at Bushland, Texas, during May and July 1992. The following were collected: diurnal radiation; evaporation (directly measured by large weighing lysimeters); five-level micrometeorological profiles of wind speed, air temperature, and relative humidity; soil temperature and volumetric water content; soil heat flux; optical turbulence (scintillometer); and near- and far-field infrared imager data over wet and dry bare soil for clear and cloudy sky conditions. Initial results from the modeling efforts indicate excellent agreement between measured and modeled values of radiation/energy balance fluxes and C_n^2, for one day. Future model evaluation will extend over the wide range of conditions encountered during the field study.

1. Introduction

Understanding surface radiation/energy balance processes is important for estimating evaporation rates and understanding surface-layer temperature and moisture gradient structure. Both the Department of Defense (DoD) and the U.S. Department of Agriculture (USDA) are interested in the development of numerically efficient methods or models to describe the partitioning of the net radiative flux into sensible, latent, and soil heat fluxes and the impact of surface fluxes on atmospheric profile structure. To make efficient use of limited fiscal and personnel resources, an integrated, multiagency effort was initiated to collect new and modern data in order to be able to improve current models. This cooperative DoD–USDA research-oriented field program, the Radiation and Energy Balance Experiment for Imagery and Electromagnetic Propagation (REBAL '92), was organized by the U.S. Army Atmospheric Sciences Laboratory (ASL) and the USDA Agricultural Research Service (ARS) Conservation and Production Research Laboratory (CPRL). REBAL '92 was conducted at Bushland, Texas, at the ARS/CPRL experimental site in May and July 1992. The site was chosen because of the diversity of meteorological, agricultural, and radiation sensors already in place. The planning and design phases for the experiment were influenced by the availability of direct measurement techniques for evaporation, soil temperatures, soil heat fluxes, and volumetric water content; parameters that are not readily available to the micrometeorological experimenter.

REBAL '92 was initiated to improve our knowledge base on radiation/energy balance partitioning and to characterize surface-layer micrometeorological processes over wet and dry soil surfaces. The project's goals were the following.

1. The collection of radiation, evaporation, micrometeorological profile, and optical turbulence scintillometer data over wet and dry bare soil, under clear and cloudy skies. In addition, infrared imager (i.e., IR video camera) data in a near-field/far-field configuration were collected simultaneously to characterize the effects of optical turbulence on a heated surface with an overlying grid (i.e., thermal bar pattern) to determine the temporal turbulent distortions of an imaged target (Watkins et al. 1991). Although the IR photography (in the midst of atmospheric effects and optical turbulence) was included, its particular application to image en-

Corresponding author address: Arnold Tunick, U.S. Army Research Laboratory, Battlefield Environment Directorate, Attn: AMSRL-BE-S, White Sands Missile Range, NM 88002-5501.
*Battlefield Environment Directorate (formerly U.S. Army Atmospheric Sciences Laboratory), U.S. Army Research Laboratory, White Sands Missile Range, New Mexico.
+USDA—Agricultural Research Service, Conservation and Production Research Laboratory, Bushland, Texas.
In final form 27 October 1993.
©1994 American Meteorological Society

hancement and battlefield target identification is beyond the scope of this presentation.

2. The evaluation, refinement, and verification of two energy balance models described by Evett and Lascano (1993) and Rachele and Tunick (1992).

The first of these two models was formulated to extend our knowledge of the energy balance fluxes, especially the evaporative or latent heat flux, for applications such as predicting crop water use and to improve irrigation scheduling and crop growth models. The second model directs its attention to the effects of the atmosphere that are basic to the performance of advanced, high-resolution systems and sensors, including lasers and imaging systems. This research effort attempts to derive reasonable estimations of the energy balance fluxes in order to determine the surface-layer structure of atmospheric profiles. By applying the basic Obukhov (1971) dynamic similarity of flows theory to the flux–gradient relationships as advocated by Dyer (1974) to radiation/energy balance model outputs, we can evaluate a quantitative estimate of the refractive index structure parameter. In this paper it will become very apparent that scintillometer data are critical for the ultimate verification and evaluation of the energy balance and electromagnetic propagation models.

The purpose of this paper is to present an overview of the REBAL '92 experiment including project objectives and goals, field site description, experimental layout, instrumentation, preliminary observations, and initial model results from the test dataset. An overview of a C_n^2–energy flux model is also given.

2. Site description

The test site at ARS/CPRL in Bushland, Texas (35°N, 102°W, 1170-m elevation MSL), is approximately 16 km due west of Amarillo, Texas. The topography is relatively level with a slope to the SE of less than 0.15%. There are no vertical obstructions near the field, and over 1000 m of cropped or fallow agricultural fields provided unobstructed upwind fetch in the predominant summer wind direction (SSW). Four weighing lysimeters are located in a 20-ha (hectare) field with each lysimeter centered in a 4.6-ha subfield (210 m × 225 m).

The test area (the NW and SW subfield) was a tilled, bare soil (Pullman clay loam) expanse approximately 210 m × 450 m (Fig. 1). Irrigated and dryland wheat fields (NE and SE lysimeter fields, respectively) were directly east of the test area. Prior to the July REBAL '92 study period, these wheat fields, as well as dryland wheat to the south of the test area, were harvested leaving a short stubble residue. A standard weather station was located about 220 m east of the test area. Daily average temperatures, wind speeds, and solar radiation as well as 15-min barometric pressures were measured at this station.

3. Experimental layout

Micrometeorological profile data (wind speed, air temperature, and relative humidity) were measured on an 8-m tower, shown in Fig. 2, centered in the test area. Data were collected at 0.5-, 1-, 2-, 4-, and 8-m above the surface. Six radiometers and one infrared thermometer (IRT) measured the radiation balance components at a site approximately 80 m north of the profile tower, about 15 m south of the NW lysimeter. Wind speed, wind direction, temperature, and relative humidity were also measured at the radiation site at 2 m. Table 1 contains a list of the instruments deployed in the REBAL '92 experiment.

The ASL Mobile Imaging and Spectroscopy Laboratory (MISL) trailer (Fig. 3) was located at the north end of the test area. The trailer contained the far-field imaging equipment (i.e., video cameras and recorders). A 0.94-μm scintillometer source module was

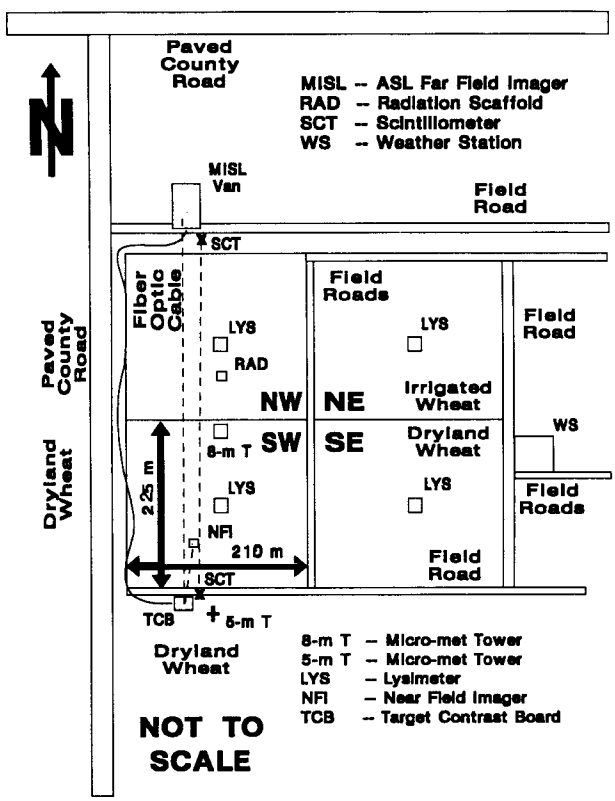

FIG. 1. The experimental test site.

TABLE 1. List of instruments* deployed in REBAL '92.

Parameter/equipment	Manufacturer/model	Deployment
8-m tower		
Air temperature/relative humidity (aspirated)	Rotronics HT225R/SMP410012	0.5, 1, 2, 4, and 8 m
Air temperature (nonaspirated)	Climatronics 100093-3	same
Wind speed	R.M. Young 12102	same
Wind direction	R.M. Young 12302	8 m
Radiation scaffold		
Incident solar radiation	Eppley PSP	1 m
Reflected solar radiation	Eppley 8-48	1 m (inverted)
Sky longwave radiation	Eppley PIR	1 m
Emitted ground radiation	Eppley PIR	1 m (inverted)
Net radiation	REBS Q*6	1 m
Total hemispherical radiation	REBS THRDS5	1 m
Surface temperature	Everest 4000	1 m [nadir; 60° FOV (field of view)]
Air temperature/relative humidity (nonaspirated)	Rotronics HT225R/SMP 41002	2 m
Wind speed	R.M. Young 12102	2 m
Wind direction	R.M. Young 12302	2 m
Lysimeter		
Reflected solar radiation	Eppley 8-48	1 m (inverted)
Net radiation	REBS Q*6	1 m
Surface temperature	Everest 4000	1 m (nadir; 60° FOV)
Soil heat flux	REBS TH-1	50 mm
Soil temperature	Thermocouples (Cu-Co)	10 and 40 mm (averaged)
Soil water	TDR (3-prong probes)/ARS-CPRL design	20 and 40 mm (averaged)
Wind speed	Met One 024	0.8, 1.3, 1.8, and 2.3 m
Dry- and wet-bulb temperature (psychrometers)	Thermocouples	1.3 and 2.3 m
Lysimeter mass	Cardinal FS-7 Scale/Alphatron SL50 load cell	

Table continued on next page →

Table 1. (Continued)

Optical turbulence/electromagnetic imaging		
Scintillometer	Lockheed Engr. & Mgmt. IV-L	N to S; 450-m path; 2 m
Visible cameras/lens	Sony NTSC DX 102s 10-power zoom lens	N to S; 50- and 450-m paths; 2 m
Infrared imagers	Inframetrics 610s/10-power lens	N to S; 50- and 450-m paths; 2 m
Target contrast board	US Army ASL	S end of field
Image recording	Analog tape	N end of field (MISL van)
Image registration	Recognition Concepts Inc.	N end of field (MISL van)
Target met tower		
Solar radiation	Qualimetrics 3120	2 m
Air temperature/relative humidity (nonaspirated)	Campbell Scientific 207	2 and 5 m
Soil temperature	Yellow Springs Instr. 703	100 mm
Barometric pressure	Intellisensor AIR-DB	2 m
Wind speed/direction	R.M. Young 05103	2 and 5 m
Visibility	HSS VF-500-100.	3 m

*The use of corporation or company names with regard to instrumentation and equipment used does not constitute an endorsement by either the U.S. Army or the USDA-ARS.

mounted 2 m above ground on a tripod located adjacent to the MISL trailer. The imaging cameras and the scintillometer were aligned and focused downfield (i.e., to the south) over a path of approximately 450 m.

The receiver module of the scintillometer, the target board (a thermally heated board with an overlying grid or bar pattern), a small storage van used as a vehicular target (i.e., an alternate IR source to photograph), and an auxiliary 5-m instrumented tower were located at the south end of the test area (Fig. 4). Instrumentation on the auxiliary tower measured 2- and 5-m elevation wind speed and direction, air temperature, relative humidity, solar radiation, barometric pressure, soil temperature (100-mm depth), and visibility near the target board to provide site-specific data for the target contrast board environment at a frequency synchronized with the imagery data.

a. Data collection summary

Micrometeorological profile data and radiation/energy balance data were collected in May 1992 (DOY 132–141) and in July 1992 (DOY 190–197). Scintillometer and infrared image data were collected during selected periods listed in Table 2 within that time frame. The field was sprinkler irrigated once on DOY 132 while significant rainfall events (i.e., more than trace rainfall) occurred on DOY 136, 141, 191, and 192. Table 2 also summarizes weather conditions during the data collection periods. Daily solar radiation data provides a good indication of daytime cloudiness or lack of cloud cover. For example, we know from personal ground observations made during the field test that DOY 134, 141, and 192 had considerable cloud cover. Additionally, two daily radiosonde observations and hourly cloud observations were recorded and four daily surface weather charts were provided during both data collection periods by the National Oceanographic and Atmospheric Administration (NOAA) National Weather Service (NWS) Office in Amarillo, Texas (about 35 km east of the field site).

b. Lysimeter measurements

The lysimeter is an intact soil monolith (3 m × 3 m square and 2.4 m deep) that can be weighed to a mass equivalent of 0.02–0.05 mm of water, which corresponds to an hourly evaporative flux of approximately

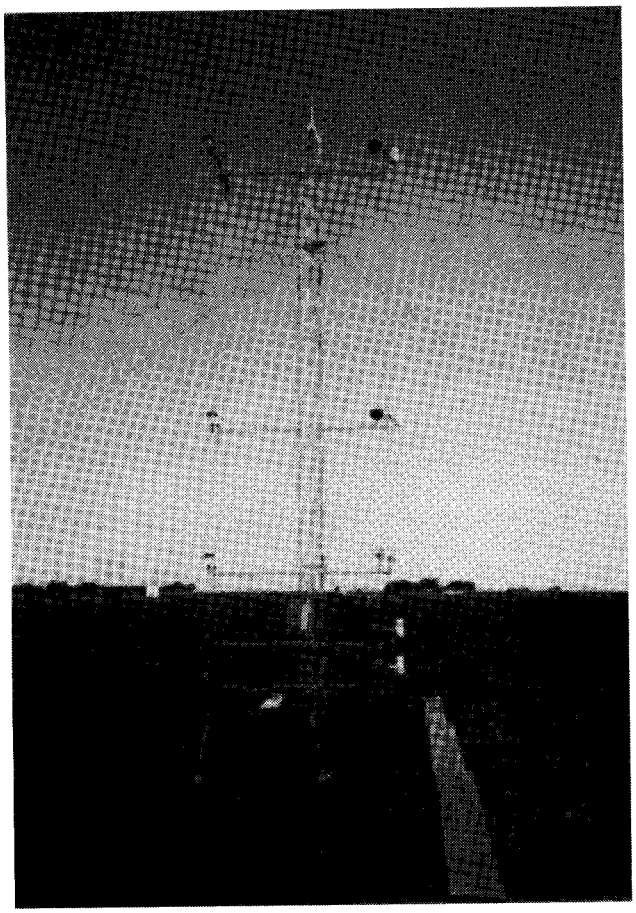

FIG. 2. The 8-m instrumented tower located at the center of the experimental site. Wind speed, wind direction, temperature, and relative humidity were measured on the mast.

14–34 W m^{-2} (Marek et al. 1988; Steiner et al. 1991). The lysimeters directly measured the water mass contained in the soil monolith. The change in this mass is the evaporation rate. The water mass was measured at 0.5-Hz frequency, averaged for 5-min periods, the difference between successive 5-min periods was averaged for 15-min periods, and these 15-min evaporation rates were smoothed using a three-point equally weighted running mean. The latent heat flux (in watts per meter^2) was computed as the product of the evaporation rate (kilograms per meter^2 per second) and the latent heat of vaporization (joules per kilogram). At each lysimeter, net radiation, reflected solar radiation, surface temperature, soil heat flux (50 mm depth), soil temperature (averaged for the 10- and 40-mm depths), wind speed profile (0.8-, 1.3-, 1.8-, and 2.3-m elevations), and dry- and wet-bulb temperatures (1.3- and 2.3-m elevations) were measured at 0.17 Hz and averaged for 15 min. Soil heat flux was corrected calorimetrically to the surface using the change in soil temperature above the plates and the soil heat capacity (Fritschen and Gay 1979).

c. Target contrast characterizer

The target contrast characterizer (TCC) compares infrared scene features collected simultaneously from an imager located near the target and from an optically matched imager located far from the target. The imagers share a common line of sight with the target, and the "near-field" images are transmitted over a video fiber-optics data cable to the far-field position for processing and recording. The "far-field" imager is coupled to a telescope of sufficient power to provide far-field images of the same dimensional field of view in the target plane as the near-field images. Pixel-to-pixel frame registration, critical to the success of this technique, is obtained through the use of a Recognition Concepts, Inc., real-time image processing system. The TCC quantifies the effect of optical turbulence on imagery by measuring the atmospheric modulation transfer function (AMTF). A target board measuring 1.78 m $\times$ 1.78 m with uniform surface temperature was used to measure the AMTF. A bar-pattern mask placed in front of the target board produced sharp hot-to-cold bar radiance transitions needed for these measurements. Video signals from visible, 3–5-μm, and 8–12-μm imagers were recorded on VHS video tape. For the REBAL '92 study, the near-field imager was placed 48 m from the target board and the far-field imager, coupled to a 10-power telescope, was placed approximately 450 m from the target board. The TCC is described in detail in Watkins et al. (1991).

d. Scintillometer measurements

A scintillometer is a ground-based, remote-sensing instrument designed to measure optical turbulence intensity along a line-of-sight path established be-

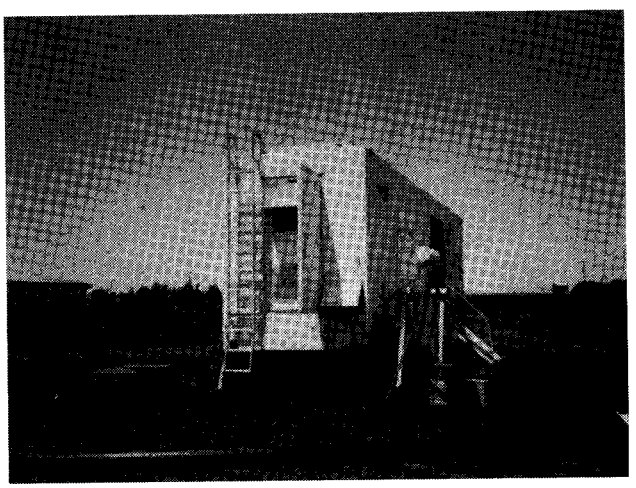

FIG. 3. The MISL trailer and the source module of the scintillometer, mounted on a 2-m tripod, were located at the north end of the field site.

TABLE 2. Summary of weather conditions during REBAL '92 in May and July 1992, Bushland, Texas.

Day of year	T_{max}* (°C)	T_{min}* (°C)	T_{dew}* (°C)	Daily solar radiation (MJ m^{-2})	Daily mean 2-m wind speed (m s^{-1})	Rain or irrigation (mm)
132+	26.4	5.4	2.3	28.3	2.4	(32.00)
133+	31.5	9.0	2.0	27.1	3.0	0.00
134+	27.9	12.4	8.5	22.9	4.4	0.00
135	30.1	11.8	7.4	26.6	3.8	0.00
136	29.8	13.4	8.2	25.2	4.1	3.05
137	26.1	11.9	7.5	25.9	4.7	0.00
138	25.0	10.6	8.3	26.0	4.8	0.00
139+	25.3	9.6	7.9	26.9	2.5	0.00
140+	26.5	11.7	8.2	25.5	3.1	0.00
141+	24.3	12.2	10.2	17.4	4.2	15.24
190+	33.9	17.7	9.2	28.7	5.3	0.00
191+	33.5	15.9	11.7	28.0	5.3	27.94
192+	30.1	17.6	15.4	24.3	4.2	6.86
193+	30.5	17.2	15.2	26.8	6.8	0.00
194	32.1	19.0	13.5	27.9	7.2	0.00
195+	31.4	17.0	12.8	25.9	3.7	0.00
196+	30.5	14.5	12.9	26.8	2.7	0.00
197	34.3	18.7	13.1	26.8	4.5	0.25

*Here, T_{max}, T_{min}, and T_{dew} are daily maximum, minimum, and mean dewpoint temperatures, respectively, measured from a standard weather shelter at 1.5-m height about 220 m east of the REBAL '92 field.
+Days when scintillometer and infrared image data were collected.

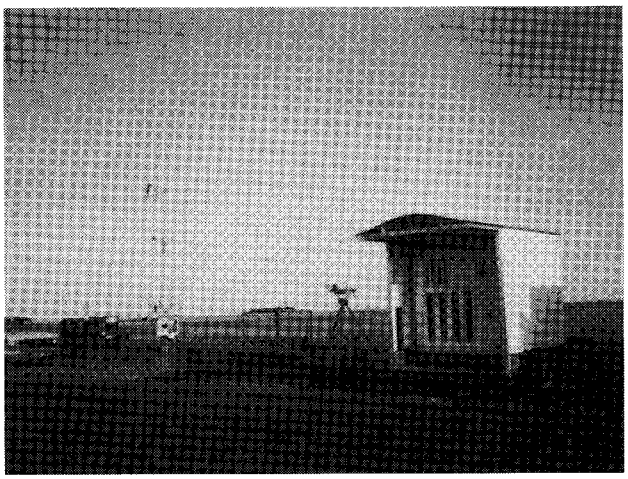

FIG. 4. The target board, source van, receiver module of the scintillometer, and an auxiliary 5-m instrumented tower were located at the south end of the field site.

tween a transmitter and a downrange receiver. Scintillometer operation is based on the principle that scintillations or light intensity variations occur as atmospheric density discontinuities create refraction effects in light propagating along a path as indicated by Clifford et al. (1974). The refractive index structure parameter, C_n^2, is related to the intensity of these refraction effects.

4. C_n^2–energy flux model

Carson (1987) defined the energy flux balance at the soil surface as

$$R_n = H + L'E + G, \quad (1)$$

where R_n is the net radiative flux, H is the sensible heat

flux, $L'E$ is latent heat flux with L' as the latent heat of vaporization (2.45×10^6 J kg^{-1}) and E as the evaporation rate in kilograms per meter^2 per second, and G is soil heat flux; units are in watts per meter^2. During REBAL '92, R_n, E, and G were measured directly (net radiometers, lysimeters, and soil heat flux plates/thermocouples, respectively), while H was computed as the residual; determined with an accuracy of about ±40 W m^{-2} or better. Carson (1987) also defined the net radiative flux at the soil surface as the sum of the net shortwave radiative flux and the net longwave radiative flux as

$$R_n = R_s - R_{sr} + R_{li} - R_{le}, \tag{2}$$

where R_s is incident solar radiation, R_{sr} is reflected solar radiation, R_{li} is sky emitted longwave radiation, R_{le} is ground emitted longwave radiation, and the units are in watts per meter^2. The shortwave reflection, albedo, is computed as R_{sr}/R_s. The effects of surface soil water content, surface roughness, and solar elevation angle on albedo is part of the REBAL '92 study along with the characterization of the net longwave radiative flux as affected by different cloud type, amount of cloud cover, and surface soil water content.

A key element of the REBAL '92 field study was the application of radiation/energy balance measurement and modeling to estimation of the intensity and character of optical turbulence as induced by atmospheric surface-layer processes. The following equations are presented in an effort to demonstrate our approach wherein the temperature and moisture flux-gradient hypothesis is applied to computations of refractive index gradients and in turn the refractive index structure parameter. While the formulations in the literature are often obscured with unnecessary complexity, the following presentation should allow those familiar with the concepts of similarity scaling constants to readily digest its content and gain some amount of appreciation for our objectives.

The refractive index structure parameter can be expressed as in Tatarski (1961):

$$C_n^2(z) = b\frac{K_H}{\varepsilon^{1/3}}\left(\frac{\partial n}{\partial z}\right)^2, \tag{3}$$

where

b = Obukhov–Corrsin constant = 3.2 (Panofsky 1968; Wyngaard 1973; Andreas 1988; Hill 1989),
ε = energy dissipation rate = $u^{*3}(\phi_m - \zeta)/kz$ (Panofsky 1968),
z = height above ground,
K_H = turbulent exchange coefficient for heat = $u^* kz/\phi_H(\zeta)$,
k = von Kármán's constant = 0.4,
u^* = friction velocity,
$\phi_H(\zeta)$ = dimensionless lapse rate = $(1-15\zeta)^{-1/2}$ for $\zeta < 0$
= $1 + 5\zeta$ for $\zeta > 0$,
$\phi_m(\zeta)$ = dimensionless wind shear = $(1-15\zeta)^{-1/4}$ for $\zeta < 0$
$\phi_m = \phi_H$ for $\zeta > 0$
(Dyer 1974; Hicks 1976),
ζ = scaling ratio = z/L,
L = Obukhov scaling length = $u^{*2}\theta/kg\theta_v^*$ (Busch 1973),
θ = potential temperature,
θ_v^* = virtual potential temperature scaling parameter,
g = gravitational acceleration,
$\partial n/\partial z$ = the gradient of the mean refractive index.

The expression we use for determining $\partial n/\partial z$ is based on expressions given by Andreas (1988). However, we modified Andreas' formulations, which are expressed in terms of temperature and *absolute* humidity gradients, to expressions in terms of potential temperature and *specific* humidity gradients as required by Tatarski (1961). For the visible region and near-infrared wavelengths from 0.36 to 3 μm (as denoted by the subscript v) Andreas (1988) writes:

$$n_v = 1 + \left\{M_1(\lambda)\frac{P}{T} + 4.615\left[M_2(\lambda) - M_1(\lambda)\right]Q\right\}10^{-6}, \tag{4}$$

where

$$M_1(\lambda) = 23.7134 + \frac{6839.397}{130 - \sigma^2} + \frac{45.473}{38.9 - \sigma^2}, \tag{5}$$

$$M_2(\lambda) = 64.8731 + 0.58058\sigma^2 - 0.007115\sigma^4 + 0.0008851\sigma^6, \tag{6}$$

where σ is λ^{-1} in micrometers, Q is absolute humidity (kilograms per cubic meter), P is pressure in millibars, and T is temperature in degrees Kelvin. Transforming Eq. (4) in terms of potential temperature (θ) and specific humidity (q) yields

$$n_v = 1 + \left\{\begin{array}{l} M_1(\lambda)\dfrac{P}{\theta - \gamma_d(z - z_r)} \quad + \\ 1.60948\left[M_2(\lambda) - M_1(\lambda)\right]\dfrac{Pq}{\theta - \gamma_d(z - z_r)} \end{array}\right\}10^{-6}, \tag{7}$$

where z_r is the reference level height and γ_d is the dry adiabatic lapse rate.

For steady-state, homogeneous conditions, Eq. (7) yields

$$\frac{\partial n}{\partial z} = \left\{-M_1(\lambda)\frac{P}{T^2} - 1.61\left[M_2(\lambda) - M_1(\lambda)\right]\frac{Pq}{T^2}\right\}10^{-6}\frac{\partial \theta}{\partial z}$$

$$+1.61\left[M_2(\lambda) - M_1(\lambda)\right]\frac{P}{T}10^{-6}\frac{\partial q}{\partial z}, \tag{8}$$

where

$$\frac{\partial \theta}{\partial z} = \frac{\theta^*}{kz}\phi_H \quad \text{and} \quad \frac{\partial q}{\partial z} = \frac{q^*}{kz}\phi_H. \tag{9}$$

In this model we use either the measured or the modeled energy fluxes of sensible heat and latent heat (Rachele and Tunick 1992) to determine the similarity scaling constants for potential temperature and specific humidity as

$$\theta^* = -\frac{H}{\rho c_p u^*}; \quad q^* = -\frac{L'E}{\rho L' u^*}, \tag{10}$$

where ρ is air density, c_p is specific heat, and L' is the latent heat of vaporization. We introduce our method for determining the surface friction velocity, u^*, which we feel is highly equivalent to the methods presented by Paulson (1970) and Benoit (1977). Our method involves an iteration whereby after an initial guess for u^* (say $u^* = 0.1\,V_r$), where V_r is the reference level total horizontal wind speed, each successive estimate is approximated by

$$u^* = \frac{V_r k}{\left[\ln\frac{x-1}{x+1} + 2\tan^{-1}(x)\right]_{z_0}^{z_r}}, \tag{11}$$

where z_0 is the roughness length and

$$x = \left(1 - 15\frac{z}{L}\right)^{1/4} \quad \text{for} \quad \frac{z}{L} < 0 \tag{12}$$

$$x = 1 + 5\frac{z}{L} \quad \text{for} \quad \frac{z}{L} > 0 \tag{13}$$

and

$$L = \frac{-u^{*3}\,\theta_{vr}\rho c_p}{k g\left(H + 0.61\,\theta_r\frac{L'E}{L'}\right)}. \tag{14}$$

In this expression for the Obukhov length, $\theta_{vr} = \theta_r(1 + 0.61 q_r)$, where the subscript r denotes the reference level (i.e., 2 m) value. It is clear that given 2-m values for sensible heat, latent heat, wind speed, temperature, and specific humidity, one can numerically determine a value for the refractive index structure parameter. Additionally, we have developed a simple method for determining the similarity scaling constants from multiple levels of discrete micrometeorological tower data (Rachele et al. 1992). The C_n^2–energy flux model can be modified to accommodate tower data gradients without significant difficulty.

5. Preliminary results

Energy balance and C_n^2 measurements on DOY 191 will be used to illustrate a portion of the data collected during REBAL '92. Figures 5 and 6 show the measured, 30-min-averaged wind speed and wind direction at 2 and 8 m, respectively, for DOY 191. Wind speeds noticeably increased about 1 h after sunrise and remained moderately strong for most of the day. Wind directions were predominantly south-southwest during DOY 191, until the onset of a thunderstorm around 1900 CST. Half-hour-averaged air temperature and dewpoint temperatures at 2-m elevation for this day are shown in Fig. 7. The maximum air temperature was close to 35.0°C. Figure 8 illustrates the observed, 30-min averaged energy balance components on DOY 191. The comparatively small magnitudes of the soil and latent heat flux components appropriately coincide with the very dry field condi-

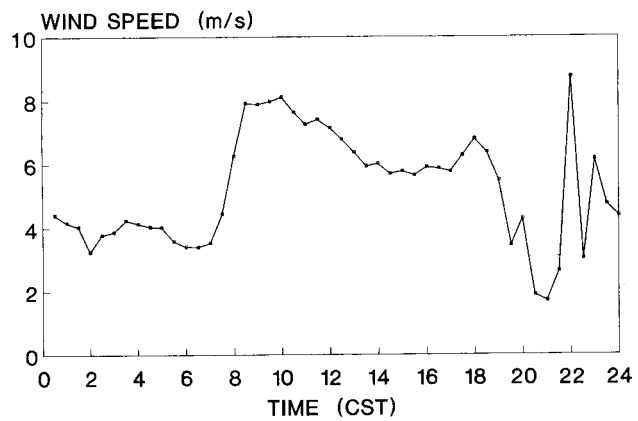

FIG. 5. Wind speed data at 2 m for DOY 191, Bushland, Texas.

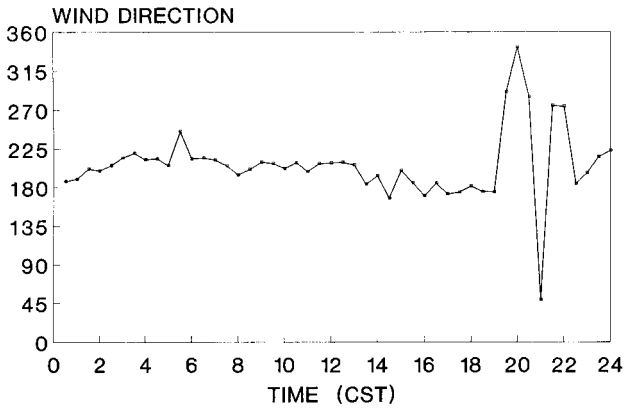

FIG. 6. Wind direction data at 8 m for DOY 191, Bushland, Texas.

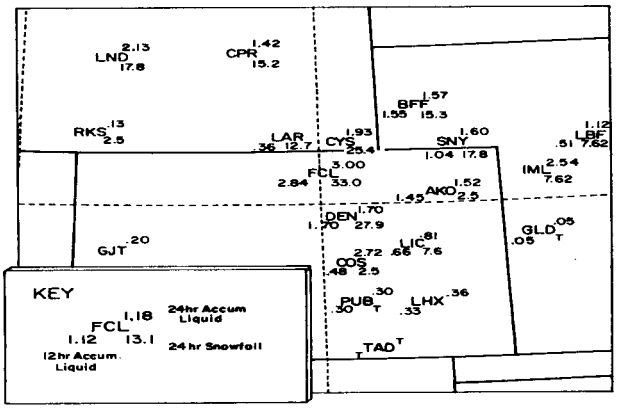

FIG. 7. Air temperature and dewpoint temperature data at 2 m for DOY 191, Bushland, Texas.

tions on this day. Figure 9 illustrates good agreement between C_n^2 measured by a scintillometer (30-min averaged data) and calculated from measured sensible and latent heat flux data [Eqs. (1–10)]. The comparison shows exceptional agreement considering the complexity of the problem. Since we assume "zero-gradient" conditions at a neutral period (i.e., a C_n^2 minimum), the measured structure parameter data suggests that the scintillometer may not have been as optimally operated as we would have liked such that a more definitive minimum "spike" would be detected. This is more often the case as reported by other optical turbulence experimenters (R. Endlich 1992, personal communication). We may conclude, however, that given reasonable values for the energy flux components, whether measured or modeled, or when deriving the temperature and moisture gradients from micrometeorological profile data, the character of the optical turbulence as represented by the refractive index structure parameter, can be accurately and quantitatively estimated.

6. Summary

A field study entitled "Radiation and Energy Balance Experiment for Imagery and E.M. Propagation" (REBAL'92) was conducted cooperatively by the U.S. Army ASL and the USDA-ARS/CPRL at Bushland, Texas, in May and July 1992. A unique set of radiation–energy balance, micrometeorological profile, scintillometer, and infrared imager data were collected over wet and dry bare soil, under clear and cloudy sky conditions. Initial evaluations indicate excellent agreement between the measured C_n^2 and estimates of the parameter using measured energy fluxes of sensible and latent heat. Modeling of the radiation–energy balance will be evaluated in future research.

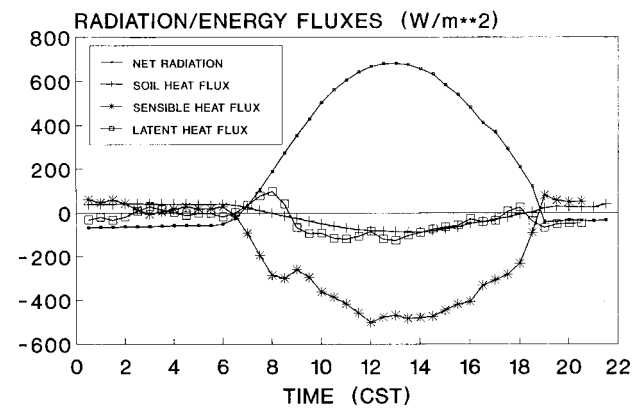

FIG. 8. Radiation and energy flux data for DOY 191, Bushland, Texas.

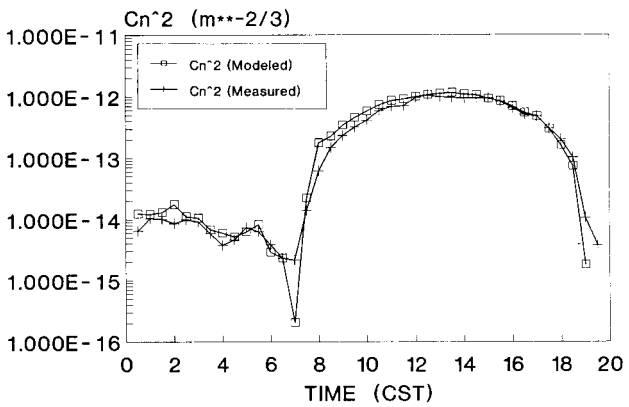

FIG. 9. Measured (at 2 m) versus modeled C_n^2 data for DOY 191, Bushland, Texas.

The utility of the newly acquired data will be vast. The nighttime micrometeorological information lends itself to initiate studies of nocturnal processes associated with energy balance. As stated in the introduction, the IR and visible video imagery has potential applications in studies of image enhancement and target identification in the midst of optically degrading atmospheric phenomena. The evaporation, soil moisture, and wind data are critical to enhancing the core of understanding related to agricultural concerns. Finally, we have completed the task of designing and executing a field program that, in and of itself, will help us to understand radiation–energy balance processes with a more pragmatic outlook.

Acknowledgments. The authors would like to thank several people for their exceptional work in the planning, execution, and support of the field project. We gratefully acknowledge Ronald Cionco, Robert Brown, Wendell Watkins, Sam Crow, Daniel Billingsley, Fernando Palacios, Don Lewis, Bob Olsen, and John Fox of the U.S. Army Atmospheric Sciences Laboratory. We also extend our thanks to B. A. Stewart, Don Dusek, Karen Copeland, and Joseph Serda of the USDA-ARS, Conservation and Production Research Laboratory. Additionally we extend our appreciation to John Eise and Steven Cooper of the NOAA, National Weather Service Office in Amarillo, Texas, and to C. L. Tate of the University of Texas, El Paso.

References

Andreas, E. L., 1988: Estimating C_n^2 over snow and sea ice from meteorological data. *J. Opt. Soc. Amer.*, **5,** 481–495.

Benoit, R., 1977: On the integral of the surface layer profile-gradient functions. *J. Appl. Meteor.*, **16,** 859–860.

Busch, N. E., 1973: On the mechanics of atmospheric turbulence. *Workshop on Micrometeorology,* D. A. Haugen, Ed., Amer. Meteor. Soc., 1–65.

Carson, D. J., 1987: An introduction to the parameterization of land-surface processes: Part 1. Radiation and Turbulence. *Meteor. Mag.*, **116,** 229–242.

Clifford, S. F., G. R. Ochs, and R. S. Lawrence, 1974: Saturation of optical scintillation by strong turbulence. *J. Opt. Soc. Am.*, **64,** 148–154.

Dyer, A. J., 1974: A review of flux-profile relationships. *Bound.-Layer Meteor.*, **1,** 363–372.

Evett, S. R., and R. J. Lascano, 1993: ENWATBAL.BAS: A mechanistic evapotranspiration model written in compiled BASIC. *Agron. J.*, **85,** 763–772.

Fritschen, L. J., and L. W. Gay, 1979: *Environmental Engineering.* Springer, 216 pp.

Hicks, B. B., 1976: Wind profile relationships from the Wangara Experiment. *Quart. J. Roy. Meteor. Soc.*, **102,** 535–551.

Hill, R. J., 1989: Implications of Monin–Obukhov similarity theory for scalar quantities. *J. Atmos. Sci.*, **46,** 2236–2244.

Lumley, J. L., and H. A. Panofsky, 1964: *The Structure of Atmospheric Turbulence.* John Wiley and Sons, Inc., 239 pp.

Marek, T. H., A. D. Schneider, T. A. Howell, L. L. Ebeling, 1988: Design and construction of large weighing monolithic lysimeters. *Trans. Am. Soc. Agri. Eng.*, **31,** 447–484.

Obukhov, A. M., 1971: Turbulence in an atmosphere with a non-uniform temperature. *Bound.-Layer Meteor.*, **2,** 7–29. [Russian original, 1946.]

Panofsky, H. A., 1968: The structure constant for the index of refraction in relation to the gradient of the index of refraction in the surface layer. *J. Geophys. Res.*, **73,** 6047–6049.

Paulson, C. A., 1970: The mathematical representation of wind speed and temperature profiles in the unstable atmospheric surface layer. *J. Appl. Meteor.*, **9,** 857–861.

Rachele, H., and A. Tunick, 1992: *Energy balance model for imagery and electromagnetic propagation.* Tech. Rep. ASL-TR-0311, U.S. Army Atmospheric Sciences Laboratory, 43 pp. [Available from U.S. Army Atmospheric Sciences Laboratory, White Sands Missile Range, NM 88002-5501.]

——, ——, and F. V. Hansen, 1992: The zephyrus, vaporous, thermotics connection. *Proc. 1992 Battlefield Atmospherics Conf.,* Ft. Bliss, TX, U.S. Army Atmospheric Sciences Laboratory, 10 pp.

Steiner, J. L., T. A. Howell, and A. D. Schneider, 1991: Lysimetric evaluation of daily potential evapotranspiration models for grain sorghum. *Agron. J.*, **83,** 240–247.

Tatarski, V. I., 1961: *Wave Propagation in a Turbulent Medium.* McGraw-Hill, 285 pp.

Watkins, W. R., S. B. Crow, and F. T. Kantrowitz, 1991: Characterizing atmospheric effects on target contrast. *Opt. Eng.*, **30,** 1563–1575.

Wyngaard, J. C., 1973: On surface-layer turbulence. *Workshop on Micrometeorology,* D. A. Haugen, Ed., Amer. Meteor. Soc., 101–149.